A fast converging adaptive control scheme for suppression of broadband disturbances on a multi-variable vibration isolation setup

G. Nijsse, J. van Dijk and J.B. Jonker
University of Twente, Faculty of Engineering Technology, Department of Mechanical Engineering,
Laboratory of Mechanical Automation, P.O. Box 217, 7500 AE, Enschede, The Netherlands
E-mail: {**G.Nijsse, J.VanDijk, J.B.Jonker**}**@CTW.UTwente.NL**

Abstract

For research and development, a single reference input multiple actuator input multiple error sensor output vibration isolation setup is realized. The objective of the setup is to investigate if the flexible receiver structure can be isolated from the rigid source structure by six piezo-electric actuators (serving as a hybrid vibration isolation mounts), such that disturbances stemming from the source structure are reduced at the receiver structure. Vibration isolation is established by minimizing signals from six acceleration sensor outputs and by steering the piezo-electric actuator inputs. The first contribution of this paper is that by making use of an adaptive multi-variable feedforward controller which is updated on the basis of a computationally efficient filtered error least mean square algorithm, broadband vibration isolation control is achieved with an average reduction of up to 9.4 dB in the error sensor outputs (between 0-1 kHz). The second contribution is that the slow convergence problem of the adaptive controller is solved by incorporating the multi-variable state space based inverse outer factor model in the control scheme. The latter is obtained from an inner/outer factorization of the state space model of the transfer path between the actuator inputs and error sensor outputs.

1 Introduction

Isolating vibrations is an important issue in a wide range of engineering applications where mechanical parts need to be connected and, at the same time, the transfer of vibration energy between the parts needs to be minimal. Vibrations can make machines less accurate, result in unwanted noise, and cause fatigue in parts of the structure or even cause damage. Examples can be found in: precision technology, transport vehicles, space and aerospace applications, biomedical applications, oil and gas platforms and buildings and constructions in a zone of seismic activity.

Vibration isolation is aimed at reducing the transmission of vibration energy from one body or structure to another. The body where the vibration originates from and the structure on which this body is mounted are called, in short, the ‘source’ and the ‘receiver’, respectively. The source - which is assumed to be rigid - needs to be appropriately connected to a receiver in order to constrain the motions of the source relative to the receiver. In this thesis, the receiver is considered to be flexible. A well-known technique to reduce the transfer of vibration energy is passive vibration isolation (PVI) by using springs and dampers (Hansen and Snyder, 1997; Mead, 1998; Preumont, 2002). The stiffness of the mount determines the fundamental resonance frequency of the mounted system and vibrations with a frequency higher than the fundamental resonance frequency are attenuated. Unfortunately, however, other design requirements (like static stability) often impose a minimum allowable stiffness, thus limiting the achievable vibration isolation by passive means. Vibrations with lower frequencies especially are difficult to isolate. Passively isolating these kinds of vibrations would result in relatively large displacements of the source. This is not desirable, as in many applications the requirements concerning the support functionality are rather strict and cannot be relaxed.

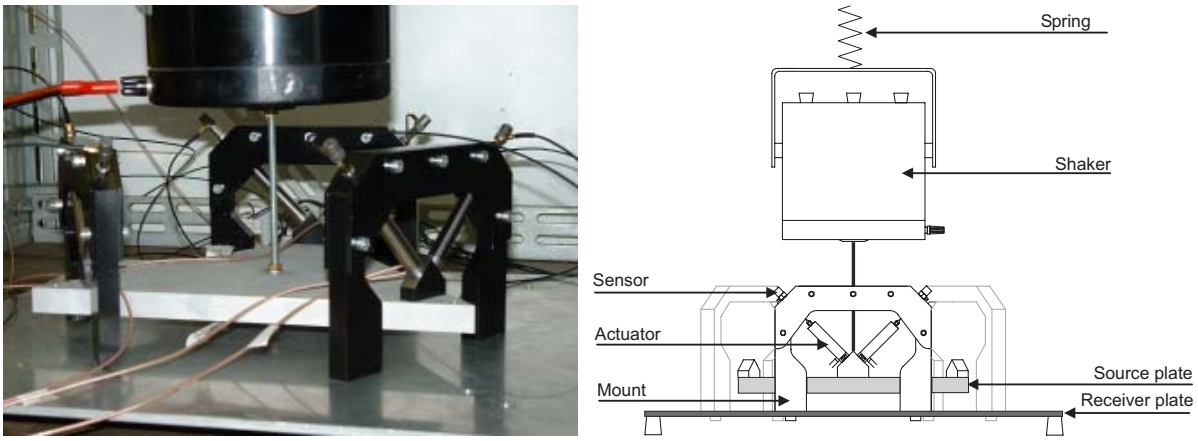

Figure 1: *The SR-MIMO vibration isolation setup (left) and a schematic representation (right).*

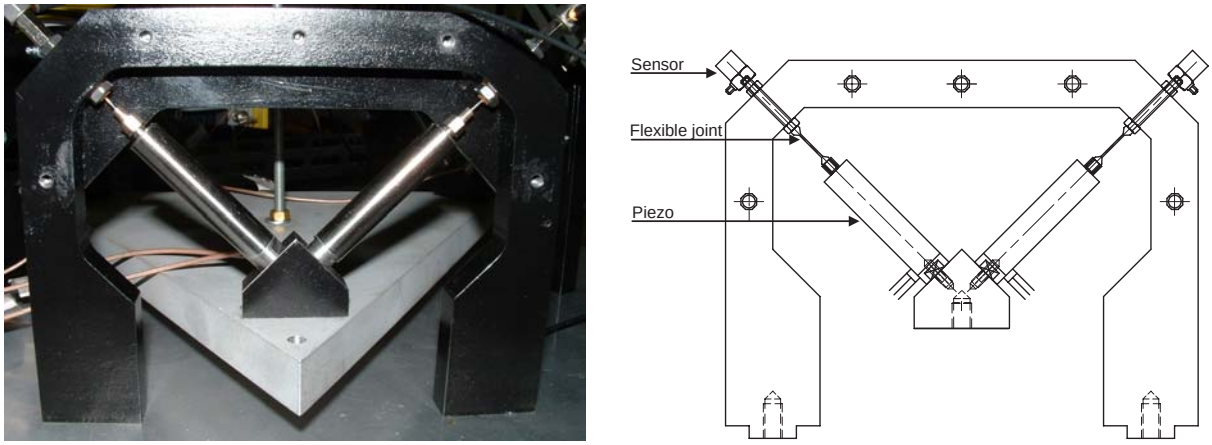

Figure 2: *One of the three mounts that carry the source (left) and a schematic representation (right). The two piezo-electric actuators can be seen clearly.*

A more promising approach to vibration isolation is statically determinate hybrid vibration isolation, which combines PVI and statically determinate active vibration isolation control (SD-AVIC) (Super, 2006). The aim of the control system in SD-AVIC is to produce anti-disturbance forces that counteract with the disturbance forces stemming from the source. Using this approach, the vibration energy transfer from the source to the receiver is blocked in the mount due to the anti-forces. For this, along with the springs and dampers, an electrical circuit is needed that consists of sensors, actuators and a real-time control system.

For research and development a single reference input multiple actuator input and multiple error sensor output (SR-MIMO) vibration isolation setup is developed (Super, 2006). In figure 1 on the left, a photograph of the SR-MIMO vibration isolation setup is shown. A schematic representation is depicted on the right. The triangular plate (i.e. the source) is excited by an electro-dynamic shaker (i.e. the reference input). The shaker is attached to a frame by a spring and moves the source dominantly in the vertical direction. The source is connected to the receiver by three hybrid mounts that consist of two piezo-electric actuators each (a mount is shown in figure 2, on the left). These mounts provide high stiffness connections in the two actuator directions and low stiffness in the unactuated directions. Thus, SD-AVIC is established in a total of six degrees of freedom (three mounts $\times$ two degrees of freedom) and PVI is established in the unactuated directions. Every mount has two error sensors that are aligned with the piezo-electric actuators. The objective of the SR-MIMO vibration isolation setup is to determine if the receiver can be isolated from the source by the vibration isolation mounts, so as to reduce disturbances stemming from the source at the receiver. SD-

AVIC is established by minimizing the signals from the six error sensor outputs and by steering the six piezo-electric actuator inputs.

The first contribution of this paper is the design, implementation and validation of a fast converging adaptive feedforward control scheme to suppress broadband disturbances in the error sensor outputs. Particularly, it is investigated if disturbances can be rejected by steering the actuators with an adaptive feedforward controller which is updated using a filtered error (adjoint) least mean squares (LMS) type of algorithm (Wan, 1996). The second contribution is that the slow convergence problem of the adaptive controller is solved by incorporating a *subspace based state space* multi-variable inverse outer factor model in the control scheme. To the inner/outer based filtered error algorithm is referred to as the IO-ALMS algorithm.

This paper is organized as follows. In section 2 the notation is explained and the IO-ALMS algorithm is given using a block-diagram. Section 3 gives the results of the simulation and real-time control experiments. Finally, in section 4 the conclusions of this paper are given.

2 Notational issues and the control scheme

This section is organized as follows. Section 2.1 clarifies the notation which is used in this paper. Section 2.2 explains the IO-ALMS algorithm. Note that in this section only the prerequisites are treated which are necessary to understand the remainder of the paper. Consult (Nijsse, 2006) and the references there-in for more in-depth information.

2.1 Notational issues

$\mathbf{Y}(q^{-1})$ is a linear time invariant transfer function with q^{-1} the unit delay operator (Fuller et al., 1996). For a state space model with system matrices $(\mathbf{A}_y, \mathbf{B}_y, \mathbf{C}_y, \mathbf{D}_y)$ it holds that the transfer function is given by $\mathbf{Y}(q^{-1}) = \mathbf{D}_y + q^{-1}\mathbf{C}_y \left(\mathbf{I}_n - q^{-1}\mathbf{A}_y\right)^{-1} \mathbf{B}_y$ with n the order of $\mathbf{Y}(q^{-1})$ and $\mathbf{I}_n \in \mathbb{R}^{n\times n}$ the identity matrix. From now often the argument q^{-1} is dropped in the equations. A hat on top of a variable (i.e. $\widehat{\{\cdot\}}$) indicates an estimate. For example, $\widehat{\mathbf{E}}$ is the estimate of $\mathbf{E}$. Furthermore, matrices, models and systems are denoted by boldface uppercase letters ($\mathbf{X}$), vectors are denoted by boldface lowercase letters ($\mathbf{x}$) and scalar signals will be denoted by normal lowercase letters (x). It is assumed that the setup is linear time invariant as well as that the reference input is stationary and broadband[1] between 0-1 kHz. Specifically, later on in the experiments, for the reference input zero mean stochastic white noise is used.

2.2 The inner/outer based adjoint least-mean-square control scheme

The control scheme is depicted in figure 3. This block-diagram is used to explain the algorithm. $\mathbf{P}$ represents the asymptotically stable[2] J input M output transfer path from the reference inputs $\mathbf{x}(k) \in \mathbb{R}^J$ to the disturbance outputs $\mathbf{d}(k) \in \mathbb{R}^M$, i.e. the primary path. The signal $\mathbf{d}(k)$ is given by:

$$\mathbf{d}(k) = \mathbf{P}\mathbf{x}(k).$$

$\mathbf{S}$ is the asymptotically stable K input M output transfer path from the actuator inputs $\mathbf{u}(k) \in \mathbb{R}^K$ to the anti-disturbance outputs $\mathbf{y}(k) \in \mathbb{R}^M$, i.e. the secondary path. Therefore:

$$\mathbf{y}(k) = \mathbf{S}\mathbf{u}(k).$$

[1] A broadband disturbance is a disturbance which is random in character and which distributes its energy evenly across a particular frequency band (Kuo et al., 1996).

[2] All poles strictly inside the unit circle.

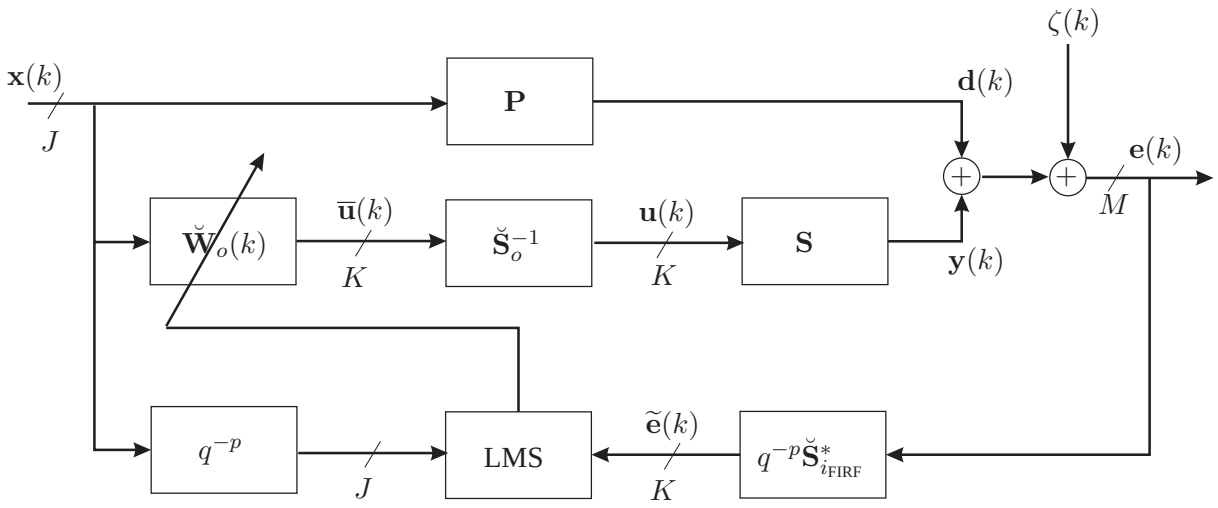

Figure 3: *Block diagram of a MIMO feedforward SD-AVIC system with an adaptive controller and the inverse outer factor included. Signals entering and leaving a plus sign ('+') have the same dimension.*

The error sensor outputs are given by $\mathbf{e}(k) \in \mathbb{R}^M$ and are a superposition[3] of the disturbance outputs $\mathbf{d}(k)$, the anti-disturbance outputs $\mathbf{y}(k)$ and the measurement noise $\zeta(k)$:

$$\mathbf{e}(k) = \mathbf{d}(k) + \mathbf{y}(k) + \zeta(k).$$

The measurement noise $\zeta(k)$ is assumed to be uncorrelated to the reference inputs $\mathbf{x}(k)$ and the disturbance outputs $\mathbf{d}(k)$. It is assumed that $M \geq K \geq J$. $\breve{\mathbf{W}}_o(k)$ is the asymptotically stable J input K output regularized adaptive feedforward controller from the reference inputs $\mathbf{x}(k)$ to $\overline{\mathbf{u}}(k)$:

$$\overline{\mathbf{u}}(k) = \breve{\mathbf{W}}_o(k)\mathbf{x}(k).$$

The controller has a finite impulse response filter (FIRF) structure of length L. The $K \times J \times L$ time-dependent coefficients of the controller are stacked in a column vector which is denoted by $\mathbf{w}_o(k)$ (Enden, 1989). $\breve{\mathbf{S}}_o^{-1}$ is the regularized[4]. K input K output inverse outer factor which is obtained from an inner/outer factorization of the augmented secondary path (Elliott, 2000; Fraanje, 2004).

$$\begin{bmatrix} \mathbf{S} \\ \sqrt{\varpi} \end{bmatrix}.$$

Specifically, $\breve{\mathbf{S}}_o$ is determined so that it holds true that:

$$\breve{\mathbf{S}}_o^* \breve{\mathbf{S}}_o = \mathbf{S}^* \mathbf{S} + \varpi \mathbf{I}_K, \tag{1}$$

with $\varpi \in \mathbb{R}^+$ a small constant. The inclusion of the regularized inverse outer factor in the control scheme can considerably speed up the convergence speed of the adaptive controller coefficients. Due to the inclusion of the regularized inverse outer factor, the adaptive feedforward controller $\breve{\mathbf{W}}_o(k)$ acts on $\breve{\mathbf{S}}_i$ which is given by:

$$\breve{\mathbf{S}}_i = \mathbf{S}\breve{\mathbf{S}}_o^{-1}.$$

Due to its computational efficiency, the least mean square (LMS) algorithm is used for updating the adaptive controller coefficients. For updating the coefficients it is necessary to compensate for the remaining inner

[3]Some authors use a minus, but here a plus is used to give $\mathbf{d}(k) + \mathbf{y}(k)$, since in real life signals are always added.

[4]The reason that the (inverse) outer factor is regularized is to prevent actuator saturation and to increase the robustness of the adaptive controller (Nijsse et al., 2005).

factor $\breve{\mathbf{S}}_i$ in the LMS algorithm. Instead of filtering the reference signal with the inner factor $\mathbf{S}_i$ in the Kronecker sense, as in the traditional filtered-x LMS algorithm (Widrow and Walach, 1996), here is chosen to filter the error sensor outputs $\mathbf{e}(k)$ with the adjoint $\breve{\mathbf{S}}_i^*$ of $\breve{\mathbf{S}}_i$. A problem is that $\breve{\mathbf{S}}_i^*$ is a state space filter (SSF) which is anti-causal and cannot be implemented in real-time. To solve this problem, $\breve{\mathbf{S}}_i^*$ is converted to a FIRF of finite length p. The FIRF is denoted by $\breve{\mathbf{S}}_{i_{\text{FIRF}}}^*$. Though $\breve{\mathbf{S}}_{i_{\text{FIRF}}}^*$ is still anti-causal, this can easily be solved by incorporating a delay of p samples. That makes the FIRF causal and thus implementable. As such, the delayed FIRF $q^{-p}\mathbf{S}_{i_{\text{FIRF}}}^*$ is used to filter the error sensor outputs $\mathbf{e}(k)$. The number p needs to be chosen with care. Making p too small may result in performance degradation.

This results in the following filtered error sensor outputs $\widetilde{\mathbf{e}}(k)$ that are actually used in the LMS update (see figure 3):

$$\widetilde{\mathbf{e}}(k) = q^{-p}\breve{\mathbf{S}}_{i_{\text{FIRF}}}^*\mathbf{e}(k). \tag{2}$$

Since the error sensor outputs $\mathbf{e}(k)$ are delayed by p samples, the reference inputs also need to be delayed by p samples. The resulting IO-ALMS algorithm is now given by:

$$\breve{\mathbf{w}}_o(k+1) \quad = \quad (1-\mu\rho)\breve{\mathbf{w}}_o(k) - \mu\mathbf{X}(k-p)\widetilde{\mathbf{e}}(k), \tag{3}$$

μ is the step-size which is chosen by the user en ρ is a small positive regularization factor to make the adaptive controller more robust too e.g. finite precision errors. $\mathbf{X}(k-p)$ a delayed version of the regression matrix $\mathbf{X}(k) \in \mathbb{R}^{JKL\times K}$ and is defined as:

$$\mathbf{X}(k-p) = \begin{bmatrix} \overline{\mathbf{x}}(k-p) & \mathbf{0} & \cdots & \mathbf{0} \\ \mathbf{0} & \overline{\mathbf{x}}(k-p) & \cdots & \vdots \\ \vdots & \mathbf{0} & \ddots & \mathbf{0} \\ \mathbf{0} & \cdots & \mathbf{0} & \overline{\mathbf{x}}(k-p) \end{bmatrix},$$

with $\overline{\mathbf{x}}(k-p) \in \mathbb{R}^{JL}$ the regression column vector that is defined as:

$$\overline{\mathbf{x}}(k-p) = \left[\overline{\mathbf{x}}_1^T(k-p)\ \overline{\mathbf{x}}_2^T(k-p)\ \cdots\ \overline{\mathbf{x}}_J^T(k-p)\right]^T,$$

with:

$$\overline{\mathbf{x}}_i(k-p) = \left[x_i(k-p)\ x_i(k-p-1)\ \cdots\ x_i(k-p-L+1)\right]^T,$$

the regression column vector of the j^{th} reference input for ($j = 1, \ldots, J$).

3 Simulation and real-time experiments

In this section simulation experiments are described which are performed in Matlab, and real-time experiments are described which are performed on an uni-processor dSPACE 1005 system. In this chapter there is focussed on the setup under consideration, which has one reference input, six actuator inputs and six error sensor outputs. Referring to figure 3 this means that $J = 1$ and $M = K = 6$. Before the discussion on the experiments is started, it is explained how the models in the control scheme are obtained.

3.1 Models which are used in the control scheme

For the adaptive control scheme a model of the secondary path is necessary. This model is necessary to be able to determine the regularized inverse outer factor model $\breve{\mathbf{S}}_o$ and the regularized inner factor $\breve{\mathbf{S}}_i$. In (Nijsse, 2006; Nijsse et al., 2005) the identification of both the primary path and the secondary path was explained in detail by using the black-box past output multi-variable output error subspace model identification (SMI) algorithm (Van Overschee and De Moor, 1994; Verhaegen, 1994). Therefor, in this paper the identification is not explained. It is only mentioned that an accurate linear model is found from raw input/output data from the setup.

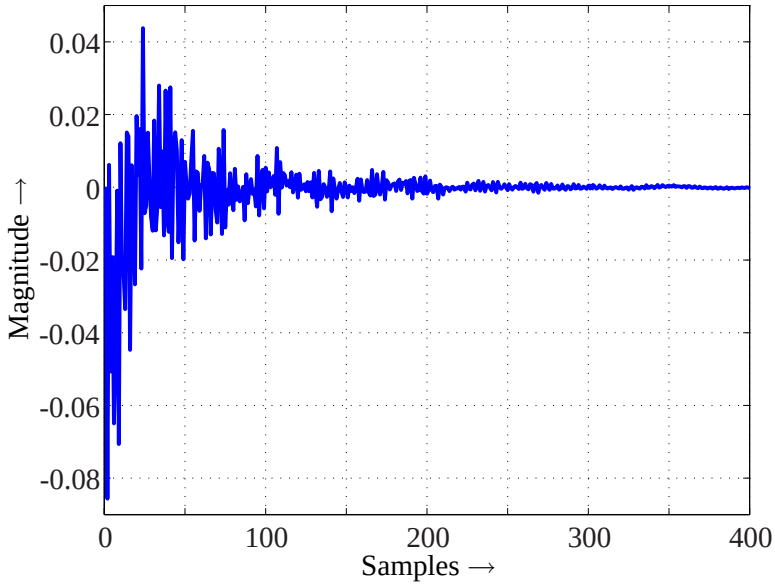

Figure 4: *Impulse response of* $\breve{\mathbf{W}}_o$ *from the first input to the first output.*

3.2 Simulation experiments

The identified models of the primary and secondary path are used to represent their true counterparts in simulation. The regularized outer factor model from equation (1) is determined with $\varpi = 0.06$ and inverted to obtain the inverse outer factor model. The regularization parameter is determined after careful analysis en multiple experiments. The adaptive controller $\breve{\mathbf{W}}_o(k)$ is regularized with a factor $\rho = 3.0 \cdot 10^{-4}$ as given in equation (3). Note that it is necessary to regularize the (inverse) outer factor model. Only regularizing $\breve{\mathbf{W}}_o(k)$ with a factor ρ would require such a high regularization parameter that the performance of the adaptive controller would be considerably decreased. A reduction of more than 2 dB on average cannot be obtained in the error sensor outputs. Performing control experiments without the inverse outer factor model included in the control scheme is possible but would result in extremely slow convergence. Converging would literally takes days.

The number of adaptive controller coefficients in each of the six channels of the adaptive controller $\breve{\mathbf{W}}_o(k)$ is obtained by examining the impulse response of the fixed gain controller $\breve{\mathbf{W}}_o$. Refer to (Nijsse et al., 2005) for techniques on how the fixed gain controller can be determined. In figure 4 the impulse response of $\breve{\mathbf{W}}_o$ is shown from the first input to the first output. The other five impulse responses are omitted for reasons of conciseness. After analyzing the impulse response, it is determined that the adaptive controller length has to be of $L = 200$. More coefficients could not be implemented on the dSPACE system due to computational limitations. Choosing $L = 200$ means that a total $6 \times 200 = 1200$ coefficients have to be adapted at every sampling instant.

Due to the regularization, a low eigenvalue-spread in the auto-correlation matrix of the filtered reference inputs of order 10^2 is accomplished (Elliott, 2000). Low, that is, considering that the eigenvalue-spread is of order 10^5 if regularizing with ρ only and of order 10^3 if regularizing with ϖ only. The regularized adjoint inner factor model $\breve{\mathbf{S}}^*_{i_{\text{FIRF}}}$ is used to filter the error sensor outputs and is described by 6×6 FIRFs. The number of coefficients p in equation (3) is derived by examining the impulse response of the regularized adjoint inner factor model $\breve{\mathbf{S}}^*_i$. Figure 5 shows one of the 36 impulse responses of $\breve{\mathbf{S}}^*_i$. Based on the impulse response, a value of 100 is chosen for the parameter p, so that $\breve{\mathbf{S}}^*_{i_{\text{FIRF}}}$ consists of $6 \times 6 \times 100$ coefficients. To save space the other 35 impulse responses are not shown. The step-size μ in the IO-ALMS algorithm in equation (3) is found to be 0.01. The reduction in the error sensor outputs after 300 seconds of convergence is shown in table 1. It appears that the performance is in accordance with the performance of the fixed gain controller,

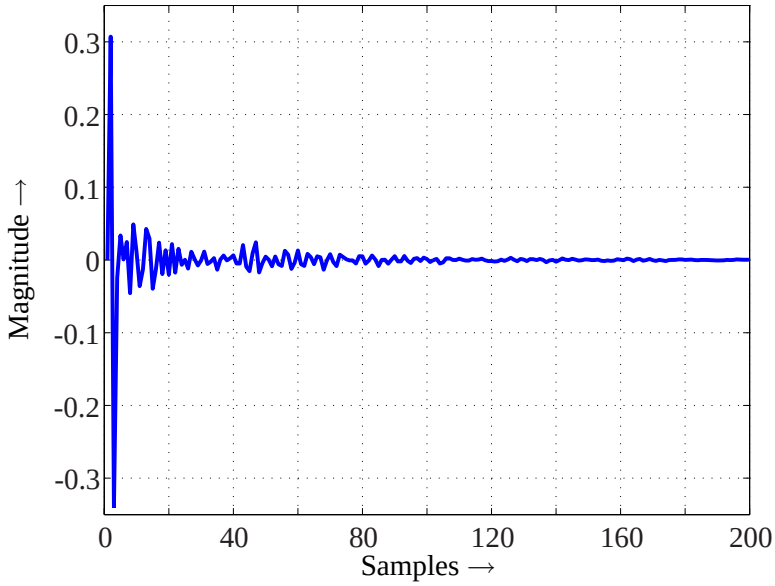

Figure 5: *Impulse response of* $\widehat{\mathbf{S}}_i^*$ *from the first input to the first output.*

Table 1: *The reduction in dB within the six error sensor outputs that are obtained in simulation with the regularized adaptive feedforward controller (second row) and fixed gain controller (third row).*

	Sensor 1	Sensor 2	Sensor 3	Sensor 4	Sensor 5	Sensor 6	Average
Adaptive:	11.7	12.6	8.9	8.4	9.1	11.1	10.3
Fixed gain:	11.8	12.7	9.1	8.9	9.5	11.1	10.5

of which the results are stated in the third row for completeness: 10.3 dB for the adaptive controller versus 10.5 dB for the fixed gain controller. On the left, figure 6 shows the performance of the controller in the first error sensor output. The results for the other five error sensor outputs are not shown here for reasons of conciseness, but these displayed similar behavior. The solid line represents the error sensor output with the controller switched off, which means that only the disturbance output contaminated with the measurement noise is present in the error sensor output. The dashed line shows the error sensor output if the controller is switched on. As these results make clear, over the entire frequency range from 0-1 kHz the disturbance output is suppressed. It can be noted that the adaptive controller is not active in the low-frequency region. That has to do with the regularization which we performed. On the right, figure 6 shows a learning curve that indicates how fast the adaptive controller coefficients converge. Within approximately 40 seconds, the adaptive controller coefficients converge close to their optimum value.

3.3 Real-time experiments

With these simulation results in mind, the adaptive controller is implemented on the real-time setup. The results are shown in table 2. The performance of the adaptive controller is 0.4 dB better than the performance of the fixed gain controller in real-time, which is understandable. The fixed gain controller is dependent on models of both the primary and secondary path. These two models both contain model uncertainty. The adaptive controller is only dependent on the regularized inverse outer factor model and the regularized inner factor model. Both of these models stem from the secondary path model only, which means less uncertainty and thus slightly better results. Figure 7 presents the performance of the controller obtained in the first error sensor output. The results are in close agreement with the simulation results (see figure 6 for comparison)

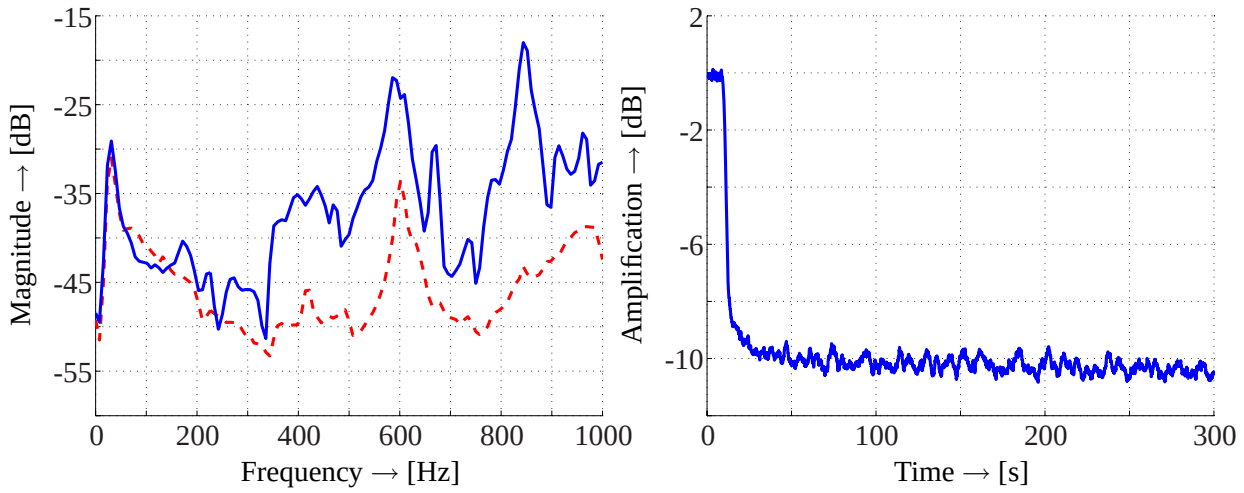

Figure 6: *Performance of the regularized adaptive feedforward controller in simulation. Left: Spectrum of the first error sensor output with (dashed, [- -]) and without (solid, [—]) control. Right: Learning curve in the error sensor outputs.*

Table 2: *The reduction in dB within the six error sensor outputs that are obtained in real-time with the regularized adaptive feedforward controller (second row) and fixed gain controller (third row).*

	Sensor 1	Sensor 2	Sensor 3	Sensor 4	Sensor 5	Sensor 6	Average
Adaptive:	11.3	11.4	7.3	7.1	8.6	10.5	9.4
Fixed gain:	10.5	10.7	7.1	7.2	8.5	9.9	9.0

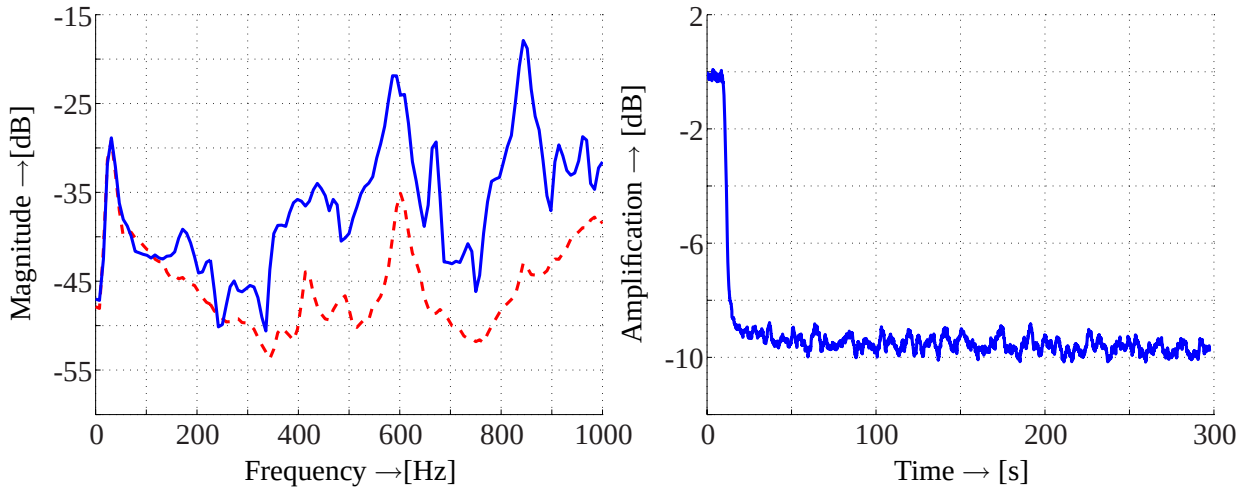

Figure 7: *Performance of the regularized adaptive feedforward controller in real-time. Left: Spectrum of the first error sensor output with (dashed, [- -]) and without (solid, [—]) control. Right: Learning curve in the error sensor outputs.*

and the fixed gain control results in both simulation and real-time. The learning curve matches the learning curve obtained from the adaptive control experiments in simulation as shown in figure 6 on the right. Within approximately 40 seconds the adaptive controller converges close to its optimum value.

4 Conclusions

In this paper the design, implementation and validation of a fast converging feedforward adaptive control scheme is described for a single reference input multiple actuator input multiple error sensor output vibration isolation setup for suppression of broadband disturbances between 0 and 1 kHz. Particularly, the adaptive controller performs well and shows a similar performance in simulation and real-time and is successfully able to reject broadband disturbances. The adaptive controller is updated with an adjoint least mean square type of algorithm. To prevent over-actuation, regularization is applied, thus robustifying the controller. The regularized adaptive controller yields a reduction of 10.3 dB in simulation and 9.4 dB in real-time. For comparison: in simulation, the fixed gain controller achieves an average reduction of 10.5 dB in the error sensor outputs. In real-time, this is 9.0 dB. Thus, the adaptive controller performs better in real-time than the fixed gain controller. This can be explained by the fact that the adaptive controller does not require information about the primary path and is able to adapt to small changes. To increase the adaptation, the state space based inverse outer factor model is included in the control scheme. This leads to convergence within a tenths of seconds.

References

Elliott, S.: 2000, *Signal processing for active control*, Academic Press.

Enden, A. V. D.: 1989, *Discrete-time signal processing*, Prentice Hall, Inc.

Fraanje, P.: 2004, *Robust and fast schemes in active noise and vibration control*, PhD thesis, University of Twente, P.O. Box 217, 7500 AE, Enschede, The Netherlands.

Fuller, C., Elliott, S. and Nelson, P.: 1996, *Active control of vibration*, Academic Press Limited.

Hansen, C. and Snyder, S.: 1997, *Active control of noise and vibration*, E & FN Spon.

Kuo, S. M., Panai, I., Chung, K. M., Horner, T., Nadeski, M. and Chyan, J.: 1996, Design of active noise control system with the TMS320 family, *Application report SPRA042*, Texas Instruments Inc., June.

Mead, D. J.: 1998, *Passive vibration control*, John Wiley and Sons.

Nijsse, G.: 2006, *A subspace based approach to the design, implementation and validation of algorithms for active vibration isolation control*, PhD thesis, University of Twente, Faculty of Engineering technology, Department of Mechanical Engineering, Laboratory of Mechanical Automation.

Nijsse, G., Super, H., Dijk, J. V. and Jonker, J.: 2005, A robust subspace based approach to feedforward control of broadband disturbances on a novel six-degrees-of-freedom vibration isolation set-up, *Noise Control Engineering Journal* **53**(5), 207–215.

Preumont, A.: 2002, *Vibration control of active structures*, second edn, Kluwer Academic Publishers.

Super, H.: 2006, *Hybrid vibration isolation of a six-degrees-of-freedom experimental setup*, PhD thesis, University of Twente, Enschede, The Netherlands.

Van Overschee, P. and De Moor, B.: 1994, N4SID: Subspace algorithms for the identification of combined deterministic and stochastic systems, *Automatica* **30**(1), 75–93.

Verhaegen, M.: 1994, Identification of the deterministic part of MIMO state space models given in innovations form from input-output data, *Automatica* **30**(1), 61–74.

Wan, E. A.: 1996, Adjoint LMS: an efficient alternative to the filtered-x LMS and multiple error LMS algorithms, *ICASSP: Proceedings of the international conference on acoustics, speech and signal processing*, Atlanta, Georgia, USA.

Widrow, B. and Walach, E.: 1996, *Adaptive inverse control*, Prentice Hall, Inc.